DOI: 10.1002/mabi.((insert number))

Article Type ((Communication))

Instructive conductive 3D silk foam-based bone tissue scaffolds enable electrical stimulation of stem cells for enhanced osteogenic differentiation[a]

John G. Hardy,* Sydney A. Geissler, David Aguilar Jr. , Maria K. Villancio-Wolter, David J. Mouser, Rushi C. Sukhavasi, R. Chase Cornelison, Lee W. Tien, R. Carmen Preda, Rebecca S. Hayden, Jacqueline K. Chow, Lindsey Nguy, David L. Kaplan* and Christine E. Schmidt*

_____

Dr. J. G. Hardy, Dr. S. A. Geissler, M. K. Villancio-Wolter, R. C. Cornelison, Prof. C. E. Schmidt
J. Crayton Pruitt Family Department of Biomedical Engineering, University of Florida, Gainesville, FL 32611, USA
Email: johnhardyuk@gmail.com (J.G.H.); schmidt@bme.ufl.edu (C.E.S.).
Dr. J. G. Hardy, Dr. S. A. Geissler, D. Aguilar Jr., D. J. Mouser, R. C. Sukhavasi, R. C. Cornelison, J. K. Chow, L. Nguy, Prof. C. E. Schmidt
Department of Biomedical Engineering, The University of Texas at Austin, Austin, TX 78712, USA
Email: johnhardyuk@gmail.com (J.G.H.); schmidt@bme.ufl.edu (C.E.S.).
Dr. J. G. Hardy, L. W. Tien, R. Carmen Preda, R. S. Hayden, Prof. D. L. Kaplan
Department of Biomedical Engineering, Tufts University, Medford, MA 02155, USA.
Email: johnhardyuk@gmail.com (J.G.H.); david.kaplan@tufts.edu (D.L.K.).

_____

Stimuli-responsive materials enabling the behaviour of the cells that reside within them to be controlled are vital for the development of instructive tissue scaffolds for tissue engineering. Herein we describe the preparation of conductive silk foam-based bone tissue scaffolds that enable the electrical stimulation of human mesenchymal stem cells to enhance their differentiation towards osteogenic outcomes.

[a] **Supporting Information** ((bold)) is available online from the Wiley Online Library or from the author.

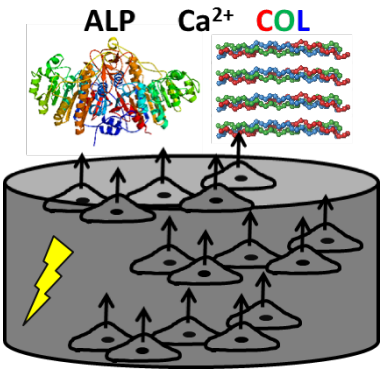

FIGURE FOR ToC_ABSTRACT

1. Introduction ((bold, 14 point font, separate all headings with an empty line))

Bone tissues are hierarchically structured composite materials composed of both soft and hard matter (i.e. cell-rich vascularized soft tissue, and collagen-/hydroxyapatite-rich hard tissue). Bone conditions and disorders that require surgical intervention motivate development of novel biomaterials that facilitate bone tissue regeneration.[1] Engineered bone tissue scaffolds to control cell outcomes in a rational fashion are of particular interest for such applications.

An incredibly diverse variety of materials have been investigated for their potential application in bone repair and regeneration,[2] including non-biodegradable materials (such as ceramics, glasses, polymethylmethacrylate and titanium)[2] or biodegradable materials (such as autografts, allografts and polycaprolactone),[2] and moreover multifunctional materials capable of drug delivery.[3] Biopolymer-based tissue scaffolds represent a particularly interesting class of biomaterials because of the versatile materials morphologies accessible via aqueous processing, and a variety of both polysaccharides and proteins have been investigated for their application as bone tissue scaffolds.[4] Natural silk proteins and recombinant silk-inspired proteins are frequently used as base materials for both drug delivery devices and tissue scaffolds with encouraging results both in vitro and in preclinical studies.[5]

Electromagnetic fields may be employed for the non-invasive stimulation of bone growth, or as invasive implantable biointerfaces such as cardiac pacemakers and neural electrodes. Biointerfaces based on conductive polymers (CPs), such as derivatives of polyaniline, polypyrrole or polythiophene, are of interest for both long term applications as low impedance coatings for electrodes with biomimetic mechanical properties and potentially for short term applications as drug delivery devices or tissue scaffolds for tissue engineering.[6]

Pro-regenerative CP-based tissue scaffolds have been developed for various tissues.[6,7] Electrical stimulation of C2C12 mouse myoblasts (a common model for muscle cells) in vitro results in increased contractile activity and maturation relative to non-stimulated controls,[8] and therefore, C2C12-adhesive polythiophene-based hydrogels with biomimetic mechanical properties represent promising muscle tissue scaffolds.[9] Likewise, electrical stimulation of peripheral nerve gaps in vivo improves the rate of recovery, thus, polypyrrole-based materials with biomimetic topographies have promise as nerve tissue scaffolds.[10]

The concept of using CP-based materials as bone tissue scaffolds was first reported by Langer and coworkers,[11] who found that applying a potential step of 20 mV/mm across 2-dimensional polypyrrole films enhanced the differentiation of bone marrow-derived stromal cells towards osteogenic outcomes, as confirmed by an increase in alkaline phosphatase (ALP) activity per cell relative to non-stimulated control substrates,[11] and further developed by others.[12] Oligoaniline-based CPs are increasingly popular biomaterials,[6i, 6j] and such polymers have been shown to promote osteogenic differentiation.[12c]

A variety of conductive protein-based materials have been prepared previously.[6g] Some examples include those based on individual components of the extracellular matrix (e.g. collagen),[13] and decellularized tissues containing a variety of extracellular matrix proteins. Additionally, functionalization of spider[14] and silkworm[15] silks with polypyrrole yields anti-static silk textiles, or novel stimuli-responsive actuators. Here we describe the preparation of conductive 3D silk foams and their use as instructive bone tissue scaffolds that enable electrical stimulation of human mesenchymal stem cells (HMSCs), thereby enhancing osteogenic differentiation (and this is to the best of our knowledge the first report of electrical stimulation on such a large scaffold).

2. Experimental Section

Full experimental details are found in the supplementary information.

3. Results and Discussion

3.1. Preparation and characterization of scaffolds

The porosity of bones varies widely, cortical canals have porosities of approximately 3.5%, whereas trabecular bones have porosities of approximately 80%, and bone tissue scaffolds typically require networks of interconnected pores with sizes of approximately 100 μm to allow for ingrowth of cells and vascularization of the scaffold.[16] Silk foams with interconnected pores with sizes greater than 100 μm (**Figure 1A**) were prepared by salt leaching (using salt particles of 425-500 μm).[17] Sacrificial templates are commonly used to impart porosity to biomaterials, and while it is possible to generate porous materials with well-defined pore interconnectivity by the removal of colloidal crystals (yielding inverse opals),[18] or 3D printed porogens,[19] our all-aqueous approach is appealing because it is cheap and scalable.[17] We rendered the scaffolds conductive by generation of an interpenetrating network of a self-doped CP within the silk foam matrix. The self-doped CPs were composed of pyrrole and 2-hydroxy-5-sulfonic aniline (**Figure 1B**),[20] and their polymerization within the silk foams was initiated by ammonium persulfate and ferric chloride.[21] When the scaffolds were homogeneously coloured, they were washed thoroughly with water and ethanol to remove the by-products that were not within or attached to the silk matrix (e.g. initiators, monomers, oligomers and polymers). The resulting conductive foams had the same pore size distributions, swell ratio and equilibrium water content as non-conductive foams (Figure 1B, **Table S1**), however, the porosity of the foams (as determined by hexane

displacement) was moderately reduced because of the presence of an interpenetrating network of the CPs within the hydrogel-like matrix of inter-/intra-molecularly crosslinked silk proteins that constitute the foam (Table S1). To within experimental error there are no differences in the mechanical properties of the materials before or after the reaction to render the scaffolds conductive; and the compressive moduli (approximately 80 kPa) and strengths (approximately 8 kPa) of the non-conductive foams and conductive foams (Table S1) would be acceptable for non-load-bearing bone tissues, and could be reinforced as necessary for load bearing tissues.[22] The conductivity of the self-doped CPs[20] was 6.1 x 10^{-4} S cm^{-1}, which is on a similar order of magnitude to those of mammalian tissues (typically $\geq 10^{-4}$ S cm^{-1}).[23]

SEM showed that the surface of the non-conductive foams are relatively smooth on the nanometer scale, whereas the conductive foams have aggregates of CP nanoparticles (composed of individual nanoparticles typically of 30-60 nm) on their surface (**Figure S1**).[20] X-ray photoelectron spectra of the non-conductive and conductive foams (**Figure 1C**) confirm that the surface chemistry of the foams has changed, with the appearance of peaks in the spectra of the conductive scaffolds at 168 eV (S 2p) and 400 eV (N 1s) resulting from the CP. Infrared spectra (**Figure 1D**) exhibit peaks at 1620 cm^{-1} and 1520 cm^{-1} corresponding to the amide I and amide II peaks, respectively, indicating the silk foam is β-sheet rich. Shoulders at 1541 cm^{-1} and 1496 cm^{-1} are characteristic of oligoanilines, and peaks at 1203 cm^{-1} (asymmetric S=O stretching), 1033 cm^{-1} (C-H in-plane deformation and/or symmetric S=O stretching), 927 cm^{-1} and a shoulder at 895 cm^{-1} (C-H out-of-plane deformation of aromatic rings and/or bipolaron bands)[20] confirm that the conductivity of the scaffolds is due to the presence of the CPs depicted in Figure 1B.

While in vitro degradation assays do not accurately reproduce patient-specific immune responses or tissue-specific enzyme distributions, they are useful to confirm the potential of materials to degrade and their relative propensities to do so. Silk proteins are well-known to degrade in vivo, and protease XIV is the most commonly used enzyme to mimic their

degradation in vitro;[24] therefore, we incubated the non-conductive and conductive foams in phosphate buffered saline (PBS) at 37 ºC in the absence or presence of protease XIV (1 U/mL) and measured their mass at specific time points (**Figure 2A**). We observed no significant mass loss for foams in the absence of the enzyme, whereas both non-conductive and conductive foams were observed to decrease in mass over the course of the experiment due to enzyme-mediated proteolysis; *in vivo* the silk component of the scaffolds is likely to degrade over the period of months to years.[24] Mass loss for the non-conductive foams was faster than for the conductive foams, which is potentially because the interpenetrating network of non-degradable CPs hinder the enzymes access to the backbone of the protein. The gradual degradation of the silk protein would leave behind a small residue of CPs. Consequently, we assessed the toxicity of the CPs using a Cell Titer-Glo® luminescent cell viability assay (**Figure 2B**). We found cell viability to be high when exposed to low concentrations (0.2 mg mL^{-1}) of CPs and to decrease above 1.5 mg mL^{-1} (a concentration greater than the mass in the individual foams), yet the CPs are markedly less toxic than nanoparticles composed of polypyrrole alone,[25] or indeed poly(3-thiophene acetic acid).[9] Silk-based materials are relatively non-immunogenic in vivo, with inflammatory responses in rats typically lower than collagen or polylactic acid,[26] as is also true of polyaniline[27] and polypyrrole[27] derivatives. Hence, we conclude that, while imperfect, such CPs represent valuable lead structures for the future development of conductive biomaterials.

3.2. In vitro cell culture

With a view to the application of the foams as bone tissue scaffolds, we seeded bone marrow-derived HMSCs[28] in the scaffolds and cultured them in osteogenic medium for up to 30 days. Three conditions were considered: 1) cells seeded on non-conductive silk foams, 2) cells seeded on conductive silk foams without electrical stimulation, and 3) cells seeded on conductive silk foams with electrical stimulation (3 days without stimulation, 6 days with stimulation at 100 mV/mm for 4 hours per day, no stimulation thereafter). In all cases, cells

adhered to the substrates and remained active for the duration of the experiments as confirmed by an AlamarBlue® assay (**Figure 2C**). As controls we seeded HMSCs on non-conductive silk foams in osteogenic medium and observed their differentiation towards osteogenic fates using biochemical assays for alkaline phosphatase (ALP) activity, Ca^{2+} deposition, collagen production (**Figure 2D to 2F**) and histology (**Figure 3A to 3F**).[29] Relative to the non-conductive silk foams ALP expression was increased on both the conductive foams with or without electrical stimulation (Figure 2D), which is likely to be a result of differences in the surface chemistry altering protein deposition from the medium onto the scaffolds.[30] Calcium deposition was increased on both the conductive foams with or without electrical stimulation, with approximately double the mass of calcium present in samples exposed to electrical stimulation after 30 days (**Figure 2E**). Likewise, collagen production was notably higher on the conductive scaffolds, and electrical stimulation markedly increased collagen production (**Figure 2F**). Thus, quantitative biochemical analyses of the scaffolds reveal that, while the non-conductive silk scaffolds support differentiation of HMSCs towards osteogenic outcomes, the application of an electrical stimulus to HMSCs residing in an conductive scaffold enhances their differentiation towards osteogenic fates, and the increased quantities of calcium and collagen are an important step towards the formation of calcified extracellular matrix associated with bone.

Histological analysis of the scaffolds (**Figure 3**) confirmed that the HMSCs differentiated towards osteogenic outcomes in all cases based on hematoxylin and eosin (H&E) staining and Alizarin staining. H&E staining of sections of non-conductive scaffolds (**Figure 3A, 3C and 3E**) resulted in characteristic blue staining of cell nuclei, and characteristic pink staining of intracellular and extracellular proteins (e.g. actin or silk, respectively).[29] Alizarin staining (**Figure 3B, 3D and 3F**) resulted in characteristic orange-red staining of calcium deposits that are early stage markers of matrix mineralization.[29c, 31] H&E staining of sections of conductive scaffolds without electrical stimulation (**Figure 3G, 3I and 3K**) or with electrical

stimulation (**Figure 3M, 3O and 3Q**) was a darker pink than the non-conductive equivalents, resulting from increased collagen production by the HMSCs on the scaffolds (Figure 2F). Likewise, Alizarin staining of sections of conductive scaffolds without electrical stimulation (**Figure 3H, 3J and 3L**) or with electrical stimulation (**Figure 3N, 3P, 3R**) was a darker red than the non-conductive equivalents, because of the increased calcium deposition in the scaffolds (Figure 2E). Qualitative analysis of the scaffolds via histology supports our quantitative biochemical analyses of the scaffolds: while the non-stimulated scaffolds support differentiation of HMSCs towards osteogenic outcomes, electrical stimulation of HMSCs enhances their biochemical phenotype.

Bone tissue engineering is a vibrant field of research, and as noted above, an incredible variety of materials have been investigated for bone tissue engineering, and silk proteins are a class of materials that has shown great promise both *in vitro* and *in vivo* in preclinical trials.[5] Herein we report the first study of a conducting silk derivative and its application as a bone tissue scaffold that facilitates electrical stimulation of HMSCs and promotes their differentiation towards osteogenic outcomes. We observe that levels of ALP expression relative to the smooth non-conductive silk foams was increased on the rougher conductive scaffolds both without and with electrical stimulation (Figure 2D). We believe that this is a result of differences in the surface chemistry altering protein deposition from the medium onto the scaffolds,[30] which Bose and coworkers show to modify cell-material interactions *in vitro*,[32] yet Epinette and Manley conclude that microstructure and surface charge are not the sole factors at play in osteoinduction in the clinic.[33] Indeed, our experimental data for non-conductive silk foams, and conductive silk foams without/with electrical stimulation enabled us to observe that electrical stimulation markedly enhanced calcium deposition and collagen production (Figure 2E, 2F and 3).

4. Conclusions

In summary, there is a need for pro-regenerative biomaterials for the treatment of bone conditions and disorders requiring surgical intervention. Engineered bone tissue scaffolds with properties that enable the behaviour of residing cells to be rationally controlled are of particular interest. We report herein the first examples of conductive 3D silk foam-based bone tissue scaffolds via a simple process under aqueous conditions and characterized their physicochemical properties. The CPs are only significantly toxic above 1.5 mg mL^{-1}, which is markedly less toxic than nanoparticles composed of polypyrrole[23] or indeed poly(3-thiophene acetic acid).[9] Moreover, the CPs reported here display markedly better electrochemical stability than poly(3-thiophene acetic acid)[9] which enabled us to electrically stimulate cells residing in the scaffolds, and we believe that the CPs represent valuable lead structures for the future development of conductive biomaterials. While there are reports of electrical stimulation of cells on 3D scaffolds composed of electrospun fibers,[34] these mats tend not to be more than 1 millimeter in thickness, and our scaffolds were 4 millimeters in height and diameter, and this is to the best of our knowledge the first report of electrical stimulation on such a large scaffold. The conductive scaffolds enable electrical stimulation of HMSCs residing therein and enhance their differentiation towards osteogenic outcomes as confirmed by both quantitative biochemical assays and qualitative histological analysis. Importantly, electrical stimulation increased quantities of calcium and collagen deposited in the scaffolds, which is an important step towards the formation of calcified extracellular matrix associated with bone.

Supporting Information

Supporting Information (full experimental details, Table S1 and additional SEM) is available from the Wiley Online Library or from the author.

Appendix/Nomenclature/Abbreviations

Acknowledgements: We thank the University of Texas at Austin for financial support in the form of a Special Research Grant to facilitate the initiation of this collaborative research project. We thank the University of Texas at Austin for financial support of David J. Mouser and Rushi C. Sukhavasi in the form of Undergraduate Research Fellowships. At the University of Austin we thank Phillip Lin for assistance with toxicity assays. SEM was carried out at the Institute for Cellular and Molecular Biology (ICMB) core lab located at the University of Texas at Austin. At the University of Florida we thank Philip Vu for assistance with degradation assays. We thank the University of Florida for financial support in the form of startup resources.

Received: Month XX, XXXX; Revised: Month XX, XXXX; Published online:
((For PPP, use "Accepted: Month XX, XXXX" instead of "Published online")); DOI: 10.1002/mabi.((insert number))

Keywords: conducting polymers; silk; stem cells; electrical stimulation; bone

[1] a) A. R. Amini, C. T. Laurencin, S. P. Nukavarapu, *Crit. Rev. Biomed. Eng.* **2012**, *40*, 363; b) J. F. Mano, G. A. Silva, H. S. Azevedo, P. B. Malafaya, R. A. Sousa, S. S. Silva, L. F. Boesel, J. M. Oliveira, T. C. Santos, A. P. Marques, N. M. Neves and R. L. Reis, *J. R. Soc. Interface*, **2007**, *4*, 999; c) A. J. Salgado, O. P. Coutinho, R. L. Reis, *Macromol. Biosci.* **2004**, *4*, 743; d) J. Ma, S. K. Both, F. Yang, F. Z. Cui, J. Pan, G. J. Meijer, J. A. Jansen, J. J. van den Beucken. *Stem Cells Transl. Med.* **2014**, *3*, 98; e) J. I. Dawson, J. Kanczler, R. Tare, M. Kassem, R. O. Oreffo., *Stem Cells.* **2014**, *32*, 35; f) Y. Liu, J. Lim, S. H. Teoh, *Biotechnol. Adv.* **2013**, *31*, 688; g) D. Marolt, M. Knezevic and G. Vunjak-Novakovic, *Stem Cell Res. Ther.* **2010**, *1*, 10; h) M. Fröhlich, W. L. Grayson, L. Q. Wan, D. Marolt, M. Drobnic, G. Vunjak-Novakovic, *Curr. Stem Cell Res. Ther.* **2008**, *3*, 254; i) W. L. Grayson, T. P. Martens, G. M. Eng, M. Radisic, G. Vunjak-Novakovic, *Sem. Cell Dev. Biol.*, **2009**, *20*, 665; j) C. A.

Lyssiotis, L. L. Lairson, A. E. Boitano, H. Wurdak, S. Zhu, P. G. Schultz, *Angew. Chem. Int. Ed.* **2011**, *50*, 200.

[2] U. G. K. Wegst, H. Bai, E. Saiz, A. P. Tomsia, R. O. Ritchie, *Nat. Mater.*, **2015**, *14*, 23.

[3] J. R. Porter, T. T. Ruckh, K. C. Popat, *Biotechnol. Prog*. **2009**, *25*, 1539.

[4] a) C. Vepari, D. L. Kaplan, *Prog. Polym. Sci*. **2007**, *32*, 991; b) S. Gomes, I. B. Leonor, J. F. Mano, R. L. Reis, D. L. Kaplan, *Prog. Polym. Sci*. **2012**, *37*, 1; c) S. Pina, J. M. Oliveira, R. L. Reis, *Adv. Mater.* **2015**, *27*, 1143; d) J. G. Hardy, T. R. Scheibel, *J. Polym. Sci. Part A: Polym. Chem.*, **2009**, *47*, 3957; e) K. Schacht, T. Scheibel, *Curr. Opin. Biotechnol.* **2014**, *29*, 62.

[5] a) S. Saha, B. Kundu, J. Kirkham, D. Wood, S. C. Kundu, X. B. Yang, *PLoS One*, **2013**, *8*, e80004; b) Z. Zhao, Y. Li, M.-B. Xie, *Int. J. Mol. Sci.*, **2015**, *16*, 4880; c) F. Vollrath, D. Porter, C. Holland, *Soft Matter*, **2011**, *7*, 9595; d) M. Widhe, J. Johansson, M. Hedhammar, A. Rising, *Biopolymers*, **2012**, *97*, 468; e) D. Pra, G. Freddi, J. Minic, A. Chiarini, U. Armato, *Biomaterials*, **2005**, *26*, 1987; f) J. G. Hardy, L. M. Römer, T. R. Scheibel, *Polymer*, **2008**, *49*, 4309; g) J. G. Hardy, A. Leal-Egaña, T. R. Scheibel, *Macromol. Biosci.*, **2013**, *13*, 1431; h) J. G. Hardy, A. Pfaff, A. Leal-Egaña, A. H. E. Müller, T. R. Scheibel, *Macromol. Biosci*., **2014**, *14*, 936; i) L. Meinel, S. Hofmann, V. Karageorgiou, C. Kirker-Head, J. McCool, G. Gronowicz, L. Zichner, R. Langer, G. Vunjak-Novakovic, D. L. Kaplan, *Biomaterials*, **2005**, *26*, 147; j) Y. Liu, R. You, G. Liu, X. Li, W. Sheng, J. Yang, M. Li, *Int. J. Mol. Sci.*, **2014**, *15*, 7049; k) S. K. Nitta, K. Numata, *Int. J. Mol. Sci.*, **2013**, *14*, 1629; l) M. Yang, Y. Shuai, W. He, S. Min, L. Zhu, *Int. J. Mol. Sci.*, **2012**, *13*, 7762; m) K.-H. Zhang, Q. Ye, Z.-Y. Yan, *Int. J. Mol. Sci.*, **2012**, *13*, 2036.

[6] a) M. Berggren, A. Richter-Dahlfors, *Adv. Mater.*, **2007**, *19*, 3201; b) J. Rivnay, R. M. Owens, G. G. Malliaras, *Chem. Mater*. **2014**, *26*, 679−685; c) T. H. Qazi, R. Rai, A. R. Boccaccini, *Biomaterials*, **2014**, *35*, 9068; d) R. Balint, N. J. Cassidy, S. H. Cartmell, *Acta*

Biomaterialia, **2014**, *10*, 2341; e) P. J. Molino, G. G. Wallace, *APL Materials*, 2015 3, 014913; f) M. Muskovich, C. J. Bettinger, *Adv. Healthcare Mater.*, **2012**, *1*, 248; g) J. G. Hardy, J. Y. Lee, C. E. Schmidt, *Curr. Opin. Biotech.* **2013**, *24*, 847; h) D. C. Martin, J. Wu, C. M. Shaw, Z. King, S. A. Spanninga, S. Richardson-Burns, J. Hendricks, Junyan Yang, *Polym. Rev*., **2010**, *50*, 340; i) B. Guo, L. Glavas, A. C. Albertsson, *Prog. Polym. Sci*., **2013**, *38*, 1263; j) D. M. Thompson, A. N. Koppes, J. G Hardy, C. E. Schmidt, *Annu. Rev. Biomed. Eng.*, **2014**, *16*, 397; k) Anthony Guiseppi-Elie, *Biomaterials*, **2010**, *31*, 2701; l) S. C. Luo, *Polym. Rev.*, **2013**, *53*, 303; m) M. A. Fernandez-Yague, S. A. Abbah, L. McNamara, D. I. Zeugolis, A. Pandit, M. J. Biggs, *Adv. Drug Deliver. Rev.*, **2015**, DOI: doi:10.1016/j.addr.2014.09.005; n) J. G. Hardy, D. J. Mouser, N. Arroyo-Currás, S. Geissler, J. K. Chow, L. Nguy, J. M. Kim, C. E. Schmidt, *J. Mater. Chem. B*, **2014**, *2*, 6809; o) D. Svirskis, J. Travas-Sejdic, A. Rodgers, S. Garg, *J. Control. Release*, **2010**, *146*, 6.

[7] a) N. K. Guimard, N. Gomez, C. E. Schmidt, *Prog. Polym. Sci*., **2007**, *32*, 876; b) A. D. Bendrea, L. Cianga, I. Cianga, *J. Biomater. Appl*., **2011**, *26*, 3.

[8] S. Ahadian, J. Ramón-Azcón, S. Ostrovidov, G. Camci-Unal, H. Kaji, K. Ino, H. Shiku, A. Khademhosseini, T. Matsue, *Biomed. Microdevices*, **2013**, *15*, 109.

[9] D. Mawad, E. Stewart, D. L. Officer, T. Romeo, P. Wagner, K. Wagner, G. G. Wallace, *Adv. Funct. Mater.*, **2012**, *22*, 2692.

[10] a) M. B. Runge, M. Dadsetan, J. Baltrusaitis, A. M. Knight, T. Ruesink, E. A. Lazcano, L. Lu, A. J. Windebank, M. J. Yaszemski, *Biomaterials*, **2010**, *31*, 5916; b) X. Liu, J. Chen, K. J. Gilmore, M. J. Higgins, Y. Liu, G. G. Wallace, *J. Biomed. Mater. Res. A*., **2010**, *94*, 1004; c) A. F. Quigley, K. J. Bulluss, I. L. Kyratzis, K. Gilmore, T. Mysore, K. S. Schirmer, E. L. Kennedy, M. O'Shea, Y. B. Truong, S. L. Edwards, G. Peeters, P. Herwig, J. M. Razal, T. E. Campbell, K. N. Lowes, M. J. Higgins, S. E. Moulton, M. A. Murphy, M. J. Cook, G. M. Clark, G. G. Wallace, R. M. Kapsa, *J. Neural Eng*., **2013**, *10*, 016008; d) J.G. Hardy, R. C. Cornelison, R. C. Sukhavasi, R. J. Saballos, P. Vu, D. L. Kaplan, C. E. Schmidt,

Bioengineering, **2015**, *2*, 15; e) C. Martin, T. Dejardin, A. Hart, M. O. Riehle, D. R. Cumming, *Adv. Healthc. Mater*., **2014**, *3*, 1001.

[11] V. P. Shastri, N. Rahman, I. Martin, R. Langer, *Mat. Res. Soc. Symp. Proc*., **1999**, *550*, 215.

[12] a) S. Meng, Z. Zhang, M. Rouabhia, *J. Bone Miner. Metab*., **2011**, *29*, 535; b) J. Pelto, M. Björninen, A. Pälli, E. Talvitie, J. Hyttinen, B. Mannerström, R. Suuronen Seppanen, M. Kellomäki, S. Miettinen, S. Haimi, *Tissue Eng. Part A*., **2013**, *19*, 882; c) J. Cao, Y. Man, L. Li, *Biomed. Rep.*, **2013**, *1*, 428.

[13] A. Blau, C. Weinl, J. Mack, S. Kienle, G. Jung, C. Ziegler, *J. Neurosci. Methods*, **2001**, *112*, 65.

[14] E. L. Mayes, F. Vollrath, S. Mann, *Adv. Mater.*, **1998**, *10*, 801.

[15] a) I. Cucchi, A. Boschi, C. Arosio, F. Bertini, G. Freddi, M. Catellani, *Synthetic Metals*, **2009**, *159*, 246; b) I. S. Romero, N. P. Bradshaw, J. D. Larson, S. Y. Severt, S. J. Roberts, M. L. Schiller, J. M. Leger, A. R. Murphy, *Adv. Funct. Mater*., **2014**, *24*, 3866.

[16] a) G. A. P. Renders, L. Mulder, L. J. Van Ruijven, T. M. G. J. Van Eijden, *J. Anat*. **2007**, *210*, 239; b) L. Cardoso, S. P. Fritton, G. Gailani, M. Benalla, S. C. Cowin, *J. Biomech*. **2013**, *46*, 253; c) V. Karageorgiou, D. Kaplan, *Biomaterials*, **2005**, *26*, 5474.

[17] D. N. Rockwood, R. C. Preda, T. Yücel, X. Wang, M. L. Lovett, D. L. Kaplan, *Nature Protocols*, **2011**, *6*, 1612.

[18] a) V. M. Swinerd, A. M. Collins, N. J. V. Skaer, T. Gheysens, S. Mann, *Soft Matter*, **2007**, *3*, 1377; b) Y. Y. Diao, X. Y. Liu, G. W. Toh, L. Shi, J. Zi, *Adv. Funct. Mater.*, **2013**, *23*, 5373; c) S. Kim, A. N. Mitropoulos, J. D. Spitzberg, H. Tao, D. L. Kaplan, F. G. Omenetto, *Nature Photon*., **2012**, *6*, 818.

[19] J. G. Torres-Rendon, T. Femmer, L. De Laporte, T. Tigges, K. Rahimi, F. Gremse, S. Zafarnia, W. Lederle, S. Ifuku, M. Wessling, J. G. Hardy, A. Walther, *Adv. Mater*., **2015**, DOI: 10.1002/adma.201405873.

[20] X. G. Li, Z. Z. Hou, M. R. Huang, M. G. Moloney, *J. Phys. Chem. C*, **2009**, *113*, 21586.

[21] R. H. Karlsson, A. Herland, M. Hamedi, J. A. Wigenius, A. Åslund, X. Liu, M. Fahlman, O. Inganas, P. Konradsson, *Chem. Mater*., **2009**, *21*, 1815.

[22] B. B. Mandal, A. Grinberg, E. S. Gil, B. Panilaitis, D. L. Kaplan, *Proc. Natl. Acad. Sci. USA*, **2012**, *109*, 7699.

[23] a) C. Gabriel, S. Gabriel and E. Corthout, *Phys. Med. Biol.*, **1996**, *41*, 2231; b) 107 S. Gabriel, R. W. Lau and C. Gabriel, *Phys. Med. Biol*., **1996**, *41*, 2251; c) S. Gabriel, R. W. Lau and C. Gabriel, *Phys. Med. Biol*., **1996**, *41*, 2271.

[24] a) Y. Cao, B. Wang, *Int. J. Mol Sci*., **2009**, *10*, 1514; b) K. Shang, J. Rnjak-Kovacina, Y. Lin, R. S. Hayden, H. Tao, D. L. Kaplan, *Transl. Vis. Sci. Technol.*, **2013**, *2*, 2; c) U. J. Kim, J. Park, H. J. Kim, M. Wada, D. L. Kaplan, *Biomaterials*, **2005**, *26*, 2775.

[25] A. Vaitkuviene, V. Kaseta, J. Voronovic, G. Ramanauskaite, G. Biziuleviciene, A. Ramanaviciene, A. Ramanavicius, *J. Hazard. Mater.*, **2013**, *250–251*, 167.

[26] L. Meinel, S. Hofmann, V. Karageorgiou, C. Kirker-Head, J. McCool, G. Gronowicz, L. Zichner, R. Langer, G. Vunjak-Novakovic, D. L. Kaplan, *Biomaterials*, **2005**, *26*, 147.

[27] M. Mattioli-Belmonte, G. Giavaresi, G. Biagini, L. Virgili, M. Giacomini, M. Fini, F. Giantomassi, D. Natali, P. Torricelli, R. Giardino, *Int. J. Artif. Organs.*, **2003**, *26*, 1077.

[28] a) G. H. Altman, R. L. Horan, I. Martin, J. Farhadi, P. R. Stark, V. Volloch, J. C. Richmond, G. Vunjak-Novakovic, D. L. Kaplan, *FASEB J*., **2002**, *16*, 270; b) J. J. Li, E. S. Gil, R. S. Hayden, C. Li, S. I. Roohani-Esfahani, D. L. Kaplan, H. Zreiqat, *Biomacromolecules*, **2013**, *14*, 2179.

[29] a) S.H. Park, E. S. Gil, H. Shi, H. J. Kim, K. Lee, D. L. Kaplan, *Biomaterials*, **2010**, *31*, 6162; b) A. Augst, D. Marolt, L. E. Freed, C. Vepari, L. Meinel, M. Farley, R. Fajardo, N. Patel, M. Gray, D. L. Kaplan, G. Vunjak-Novakovic, *J. Roy. Soc. Interface*, **2008**, *5*, 929; c)

C. Correia, S. Bhumiratana, L. P. Yan, A. L. Oliveira, J. M. Gimble, D. Rockwood, D. L. Kaplan, R. A. Sousa, R. L. Reis, G. Vunjak-Novakovic, *Acta Biomaterialia*, **2012**, *8*, 2483.

[30] H. M. Rawel, K. Meidtner, J. Kroll, *J. Agric. Food Chem.*, **2005**, *53*, 4228.

[31] P. C. Bessa, E. R. Balmayor, J. Hartinger, G. Zanoni, D. Dopler, A. Meinl, A. Banerjee, M. Casal, H. Redl, R. L. Reis, M. van Griensven, *Tissue Eng. Part C Methods*, **2010**, *16*, 937.

[32] S. Tarafder, S. Bodhak, A. Bandyopadhyay, S. Bose, *J. Biomed. Mater. Res. Part B Appl. Biomater.*, **2011**, *97B*, 306.

[33] *Fifteen years of clinical experience with hydroxyapatite coatings in joint arthroplasty*, (Eds: J.-A. Epinette, M. T. Thomas), Springer-Verlag, Paris, France **2004**.

[34] a) L. Ghasemi-Mobarakeh, M. P. Prabhakaran, M. Morshed, M. H. Nasr-Esfahani, H. Baharvand, S. Kiani, S. S. Al-Deyab, S. Ramakrishna, *J. Tissue Eng. Regen. Med.*, **2011**, *5*, e17; b) J. Y. Lee, *Polymer Reviews*, **2013**, *53*, 443.

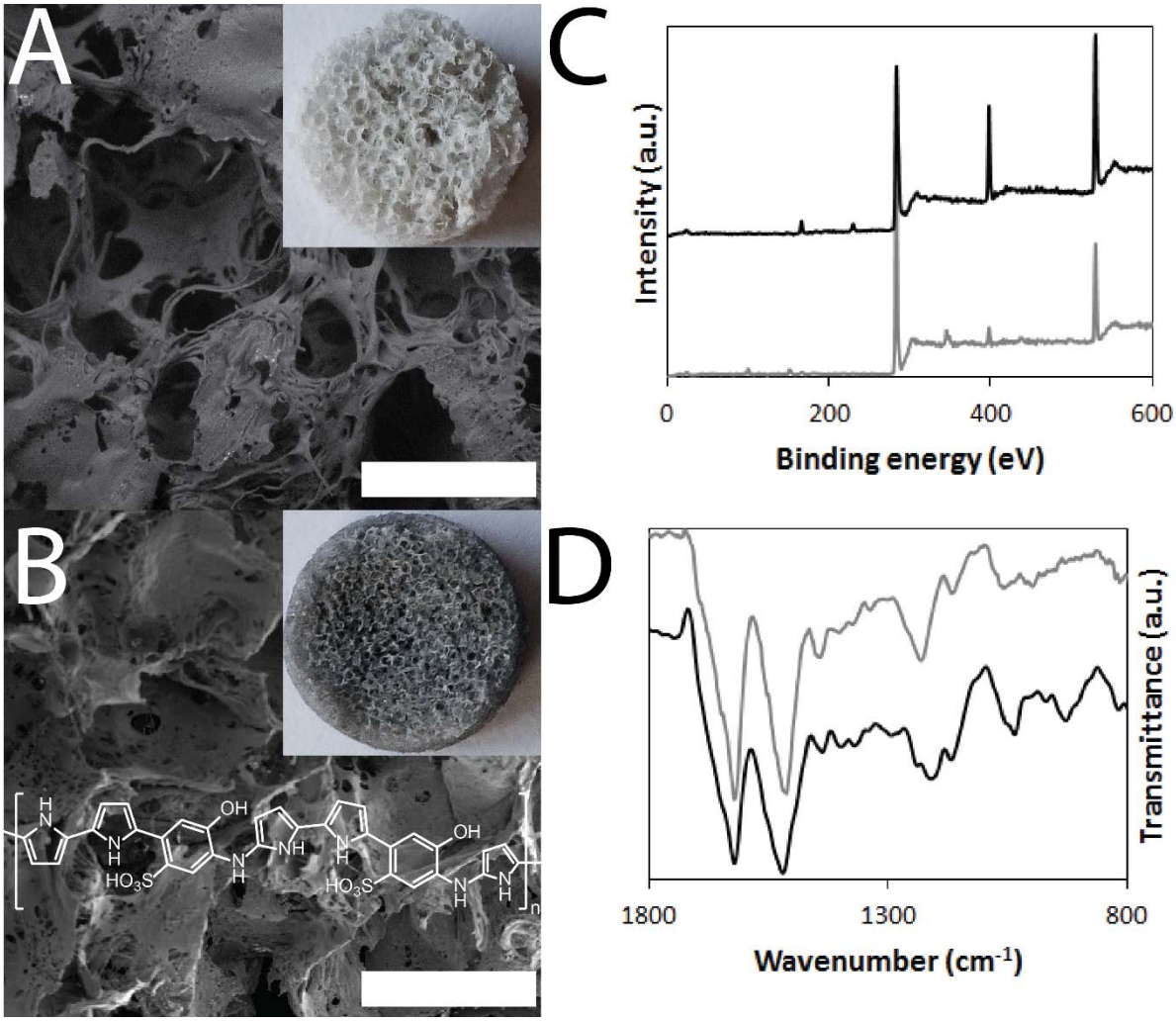

Figure 1. Physicochemical analysis of the tissue scaffolds. A) SEM image of non-conductive silk foam with inset photograph of the bulk foam. B) SEM image of conductive silk foam, with inset photograph of the bulk foam, and the structure of the self-doped CP composed of pyrrole and 2-hydroxy-5-sulfonic aniline overlaid. Scale bars represent 400 µm, and the bulk foams were 4 mm in diameter and height. C and D) XPS and FTIR spectra, respectively; grey lines represent spectra of non-conductive silk foams and black lines represent spectra of conductive silk foams. The appearance of peaks in the XPS spectrum of the conductive silk foam at 168 and 400 eV, and in the FTIR spectrum of the conductive silk foam at 1203, 1033, 927 and 895 cm-1 confirm that the surface chemistry of the silk foams changed after growth of an interpenetrating network of CPs.

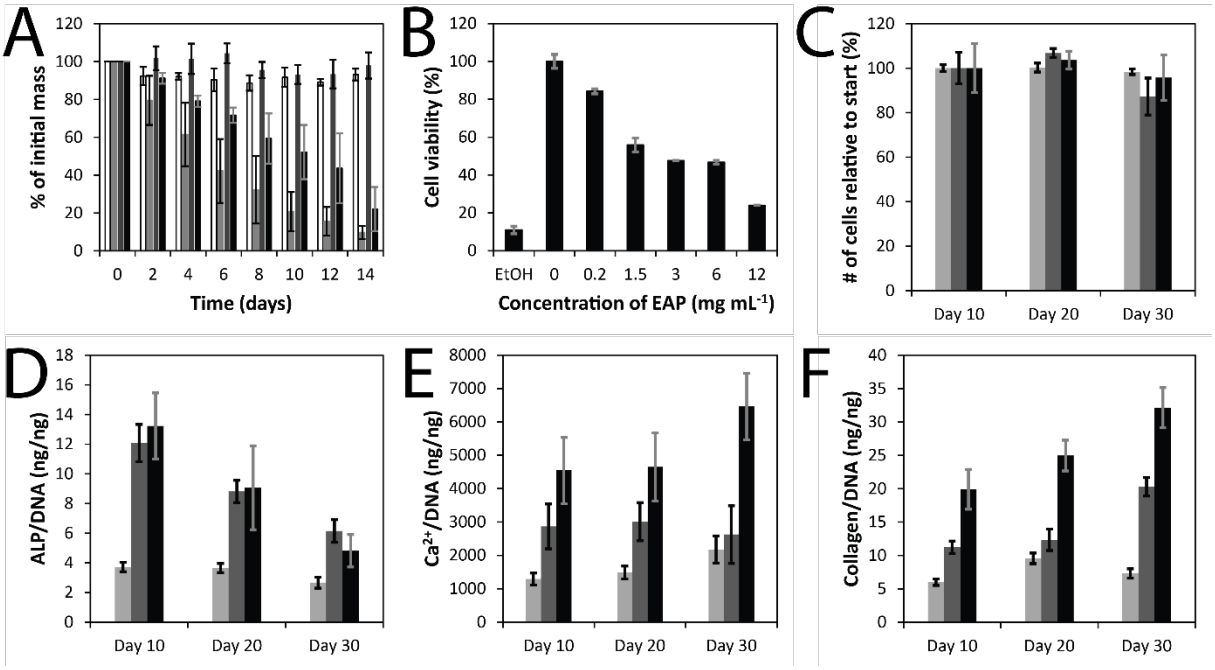

Figure 2. Biochemical analysis. A) In vitro degradation assay: white bars, silk foam without enzyme; light grey bars, silk foam with enzyme; dark grey bars, conductive silk foam without enzyme; black bars, conductive silk foam with enzyme. B) HMSC viability after incubation with ethanol (15% v/v, toxic control) or different concentrations of CP. C to F) Quantitative studies of cell culture experiments: light grey bars, silk foam; dark grey bars, conductive silk foam without electrical stimulation; black bars, conductive silk foam with electrical stimulation.

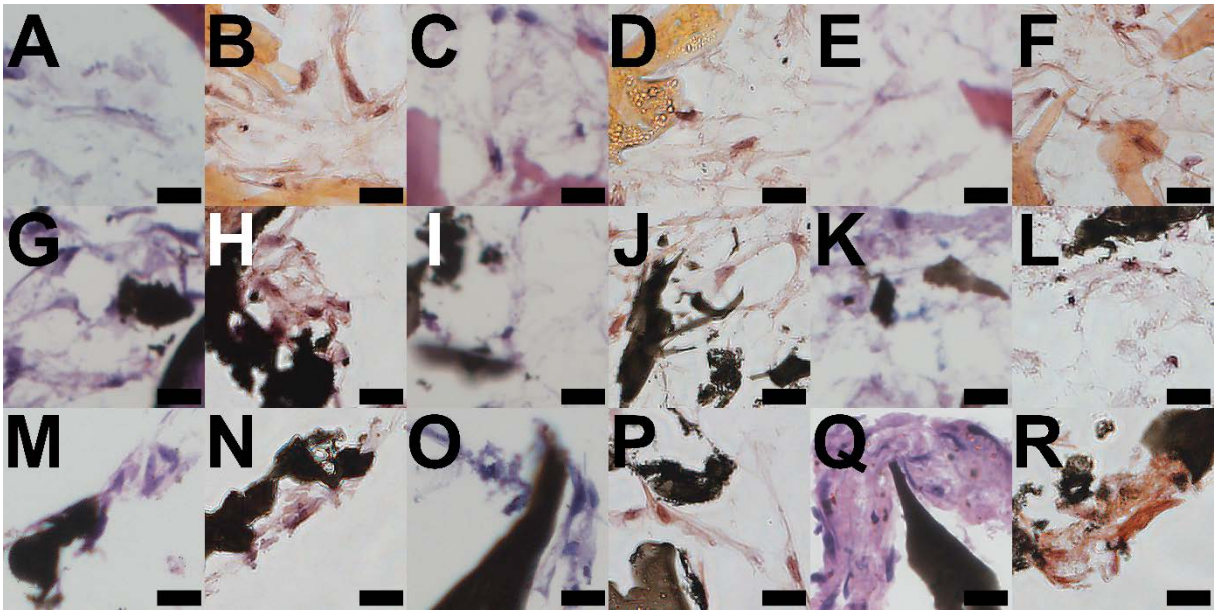

Figure 3. Histological analysis of the scaffolds at various points in time. Hematoxylin and eosin (H&E) staining of sections of non-conductive scaffolds results in characteristic blue staining of cell nuclei, and characteristic pink staining of intracellular and extracellular proteins (e.g. actin or silk, respectively); Alizarin staining results in characteristic orange-red staining of calcium deposits that are early stage markers of matrix mineralization; the CP is black. A to F: non-conductive silk foams. A) 10 days, H&E. B) 10 days, Alizarin. C) 20 days, H&E. D) 20 days, Alizarin. E) 30 days, H&E. F) 30 days, Alizarin. G to L: conductive silk foams without electrical stimulation. G) 10 days, H&E. H) 10 days, Alizarin. I) 20 days, H&E. J) 20 days, Alizarin. K) 30 days, H&E. L) 30 days, Alizarin. M to R: conductive silk foams with electrical stimulation. M) 10 days, H&E. N) 10 days, Alizarin. O) 20 days, H&E. P) 20 days, Alizarin. Q) 30 days, H&E. R) 30 days, Alizarin. Scale bars represent 100 µm.

Instructive tissue scaffolds capable of controlling the behaviour of the cells that reside within them are particularly interesting for tissue engineering. Herein we describe the preparation of conductive silk foam-based bone tissue scaffolds that enable the electrical stimulation of human mesenchymal stem cells to enhance their differentiation towards osteogenic outcomes.

J. G. Hardy,* S. A. Geissler, D. Aguilar Jr. , M. K. Villancio-Wolter, D. J. Mouser, R. C. Sukhavasi, R. C. Cornelison, L. W. Tien, R. C. Preda, R. S. Hayden, J. K. Chow, L. Nguy, D. L. Kaplan,* C. E. Schmidt*

Instructive conductive 3D silk foam-based bone tissue scaffolds enable electrical stimulation of stem cells for enhanced osteogenic differentiation